

Published in final edited form as:

*Nat Cell Biol.* 2009 January ; 11(1): 78–84. doi:10.1038/ncb1815.

## Auxin transport through non-hair cells sustains root-hair development

Angharad R. Jones<sup>1</sup>, Eric M. Kramer<sup>2,3</sup>, Kirsten Knox<sup>4,5</sup>, Ranjan Swarup<sup>3,6</sup>, Malcolm J. Bennett<sup>3,6</sup>, Colin M. Lazarus<sup>1</sup>, H. M. Ottoline Leyser<sup>4</sup>, and Claire S. Grierson<sup>1</sup>

<sup>1</sup> School of Biological Sciences, University of Bristol, BS6 6JX, UK.

<sup>2</sup> Physics Department, Bard College at Simon's Rock, Massachusetts, MA 01230, USA.

<sup>3</sup> Centre for Plant Integrative Biology, University of Nottingham, LE12 5RD UK.

<sup>4</sup> Department of Biology, University of York, YO10 5YW, UK.

<sup>5</sup> Institute of Molecular Plant Sciences, University of Edinburgh, EH9 3JR, UK.

<sup>6</sup> Plant Sciences division, School of Biosciences, University of Nottingham, LE12 5RD UK.

### Abstract

The plant hormone auxin controls root epidermal cell development in a concentration-dependent manner<sup>1-3</sup>. Root hairs are produced on a subset of epidermal cells as they increase in distance from the root tip. Auxin is required for their initiation<sup>4,7</sup> and continued growth<sup>8,11</sup>, but little is known about its distribution in this region of the root. Counter to the expectation that hair cells might require active auxin influx to ensure auxin supply, we did not detect the auxin-influx transporter AUX1 in root-hair cells. A high level of AUX1 expression was detected in adjacent non-hair cell files. Non-hair cells were necessary to achieve wild-type root-hair length, although an auxin response was not required in these cells. 3D modelling of auxin flow in the root tip suggests that AUX1-dependent transport through non-hair cells maintains an auxin supply to developing hair cells as they increase in distance from the root tip and sustains root-hair outgrowth. Experimental data support the hypothesis that, instead of moving uniformly through the epidermal cell layer<sup>3,12</sup>, auxin is mainly transported through canals that extend longitudinally into the tissue.

---

Precise temporal control of developmental processes is essential for the production of complex, repeatable cell morphologies. The root epidermis of *Arabidopsis* consists of two cell types, hair and non-hair, that are found in files that run the length of the root (Fig. 1a). Root hairs are long, thin outgrowths that emerge from the surface of epidermal cells. The specialized shape of root-hair cells is likely to be important for efficient water and nutrient uptake. Variation in environmental conditions can alter the morphology of hair cells, in the simplest instance affecting the length of the hair<sup>13</sup>. The tube-like structure of the hair is gradually extended by growth at its tip. Duration of tip growth affects the final length of the hair<sup>4</sup>.

As root-epidermal cells mature their distance from the root tip increases. Cells undergoing division, elongation and differentiation are found in longitudinal zones of the root (Fig. 1a). A concentration maximum of the plant hormone auxin is found in the root tip<sup>1</sup>. Auxin is transported in an acropetal (tipwards) direction in the stele, redistributed in the root tip and transported in a basipetal (shootwards) direction in the lateral root cap and epidermis (Fig.

1a)<sup>2</sup>. With sufficient movement of auxin from the basipetal to the acropetal stream, mathematical modelling demonstrates a reflux loop is created sufficient to establish and maintain local auxin concentrations and zonation of developmental activity in the two most apical zones of the root<sup>3</sup>. Root-hair growth is observed in the differentiation zone of the root, the most basally located developmental zone (Fig. 1a). Initiation of root-hair growth is dependent on auxin<sup>5,7</sup> and the relative amounts of two antagonistically acting *AUX/IAA* transcription factors, *AXR3* and *SHY2*, which are degraded in response to auxin<sup>4</sup>. Initiation is followed by a period of rapid outgrowth. Addition of exogenous auxin increases root-hair length, while inhibition of auxin signalling or disruption of auxin transport results in a decrease in root-hair length<sup>8,9</sup>. Experiments in which the intracellular auxin concentration of developing root-hair cells was manipulated indicate a strong positive relationship between auxin concentration and root-hair outgrowth<sup>10,11</sup>. These data suggest that the differentiation zone represents a region of the root within which spatial distributions of *AUX/IAAs* and auxin promote root-hair growth. However, little is known about the distribution or movement of auxin in this region of the root.

Auxin distribution is controlled by the movement of auxin into and out of individual cells. Protonated auxin enters cells from the cell wall by diffusion, while the ion enters via the activity of *AUX1/LAX* auxin-influx facilitators. *AUX1* activity increases efficiency of auxin uptake compared to diffusion alone, allowing accumulation and efficient transport of auxin within tissues<sup>12,14,15</sup>. At cytoplasmic pH auxin is almost completely deprotonated and as a result requires active transport to move across the plasma membrane and out of the cell. Asymmetric subcellular localization of the *PIN* family of auxin efflux carriers<sup>16</sup> therefore creates directional movement of auxin<sup>2,17</sup>. Some P-glycoproteins also have auxin-transporting capabilities<sup>11,18</sup>, but their physiological role is less clear. Although *AUX1* and *PIN2* are expressed in the root epidermis<sup>2,6,19,20</sup>, relative hair and non-hair expression levels are unclear. We studied the expression of functional *AUX1-YFP* under the control of the *AUX1* promoter (*AUX1::AUX1-YFP*)<sup>21</sup> and functional *PIN2-GFP* under the *PIN2* promoter (*PIN2::PIN2-GFP*)<sup>22</sup> in the elongation and differentiation zones of the root. Since auxin is essential for root-hair elongation and *AUX1* seems important for auxin accumulation in the epidermis<sup>12,15</sup>, the naïve expectation is that *AUX1-YFP* should be expressed at high levels in hair cells. Surprisingly, *AUX1-YFP* was undetectable above background fluorescence in hair cells, whilst strong YFP signal was observed in non-hair cells (Fig. 1b). *AUX1* expression was first observed in the epidermis as it emerges from under the root cap, from which point cell file specific stripes were visible (Fig. S1). We observed *PIN2-GFP* signal in both cell types (Fig. 1c).

Despite the absence of detectable *AUX1-YFP* in hair cells, the average root-hair length of the *aux1-22* null mutant<sup>21</sup> was shorter than wild type (Fig. 2a,b,d), but could be increased by the application of exogenous auxin (Fig. S2). This agrees with previous descriptions of mutant *aux1* alleles<sup>8,9</sup>. Transgenic expression of *AUX1-YFP* under the control of a root-hair-specific promoter has previously been shown to increase the length of root hairs<sup>11</sup> indicating that *AUX1* can directly affect root-hair length by affecting the concentration of auxin in root-hair cells. However, we found that introduction of the *AUX1::AUX1-YFP* construct, which is undetectable in hair cells, was sufficient to increase *aux1-22* root-hair length (Fig. 2c,d).

*AUX1* is expressed in the stele, where it is thought to be associated with the accumulation of auxin in the root tip<sup>19</sup>, and in the lateral root cap and epidermis<sup>19</sup> where it is essential in establishing the supply of auxin to developing epidermal cells<sup>12</sup>. Consistently, GUS expression from the auxin responsive reporter *IAA2::GUS*<sup>19</sup> was found to be more intense in the root tip<sup>12</sup> and the differentiation zone of wild-type roots than of *aux1-22* roots (Fig. 2e-f). Within the *aux1-22* genotype the most intense staining was observed in individuals

that also produced the longest hairs (Fig. S3), suggesting that one or both of the observed auxin responses may be associated with root-hair growth.

To determine whether acropetal or basipetal transport is required for root-hair growth, functional HA-tagged AUX1 was introduced into the *aux1-22* background under the control of tissue-specific promoters using a GAL4 transactivation approach<sup>12</sup>. Expressed under the control of a stele-specific promoter (*J1701*) HA-AUX1 was not able to increase the average length of *aux1-22* root hairs, but under the control of a promoter active in the lateral root cap and epidermis (*M0028*) *aux1-22* root-hair length was increased (Fig. 2g). This suggests basipetal auxin transport (*M0028*) rather than acropetal transport (*J1701*) is important for root-hair growth and indicates that the auxin response in the differentiation zone may be important. Interestingly, when expressed under a root-cap-specific promoter (*M0013*), HA-AUX1 did not increase root-hair length (Fig. 2g) indicating that AUX1 may be required in both the epidermis and lateral root cap to induce wild-type root-hair growth.

We next investigated the role of non-hair cells in the control of root-hair growth. In the *werewolf/myb23* (*wer/myb23*) mutant every epidermal cell develops as a hair cell<sup>23</sup> (Fig. 3b). Expression of the *AUX1::AUX1-YFP* construct was detected in the stele and root cap, but not the epidermis (Fig. S4). *wer/myb23* root hairs were found to be shorter than wild-type hairs (Fig. 3a-c), but increased to a length equal to wild type upon application of auxin (Fig. S5). This suggests that the length of *wer/myb23* root hairs is restricted by the loss of a promoting signal produced by non-hair cells. It has previously been shown that interaction between hair and non-hair cells is essential during the establishment of epidermal cell fate<sup>24</sup>. Our results suggest that interaction between non-hair cells and hair cells is also required to sustain root-hair development.

While non-hair cells were found to promote root-hair growth, an auxin response was not required in this cell type. The gain-of-function *axr3-1* mutation blocks auxin response in root tissues<sup>12</sup> and prevents root-hair development<sup>4,25</sup> (Fig. 3d). Expression of *axr3-1* in epidermal initials and non-hair cells using a transactivation driver line (J2301) (Fig. 3g) did not prevent root-hair initiation or growth (Fig. 3e, S6), although expression of the same construct throughout the root did (J0491) (Fig. 3 f,h, S6). Taken together with the expression pattern of AUX1 in the epidermis and the role of intracellular auxin in promoting root-hair elongation<sup>10,11</sup>, the simplest explanation of these results is that non-hair cells affect the supply of auxin to hair cells.

To predict auxin distribution in the developing epidermis we incorporated the observed *AUX1* expression pattern into a computer model of auxin transport in the elongation and differentiation zones of the root. The model simulates cells in the outer three layers of the root (Fig 4a). Auxin movement across the plasma membrane and within the cytoplasmic and apoplastic compartments is simulated, incorporating both carrier-mediated and diffusive auxin movement as appropriate. Parameter values are based on available biophysical and biochemical data as described in the Supplementary Information provided online and in the online supplement of Swarup et al 2005<sup>12</sup>. The model is an improvement of an earlier model of the root apex<sup>12</sup> in the following ways. First, each hair-cell file overlies a radial longitudinal wall separating two cortical cells. Contact with this wall, as viewed in transverse sections of the Arabidopsis root, is the major determinant of hair cell fate<sup>26</sup>. Second, AUX1-mediated influx is only present in non-hair cells. This 3D model allows the effects of lateral diffusion in the tangential plane of the tissue, essential to understanding movement between hair and non-hair cell files, to be studied.

The most prominent effect of the *AUX1* expression pattern is that non-hair cells accumulate a much higher cytoplasmic concentration of auxin than hair cells (Fig. 4b). Since the model

parameters reflect our estimate that *AUX1* allows auxin to enter cells ~10 times faster than by diffusion alone<sup>14</sup>, the concentration in non-hair cells is higher by roughly this ratio. However, since auxin can enter cells by diffusion, auxin is not completely excluded from hair cells. If the auxin source at the root apex allows for ~300 nM auxin in the non-hair cells, the concentration in hair cells is ~30 nM. This is well within the measured range of biological activity in root-hair development assays<sup>10,27</sup> (see Online Supplementary Information). Auxin flux, which is calculated as the product of auxin concentration and auxin-transport speed, will also be higher through non-hair cell files than in hair cell files. However, the small amount of flux created by the expression of PIN2 in hair cells may still be important in preventing auxin from pooling in these cells<sup>28</sup> and in determining their polarity<sup>6</sup>. Interestingly, an intracellular auxin gradient is predicted in both hair and non-hair cells.

Fig. 4c shows our model of the *aux1* mutant. Loss of AUX1 from non-hair cells means that all epidermal cells have uniform auxin transport capacity and auxin distribution in hair- and non-hair- cell files is identical. The relatively slow rate of influx allows auxin to accumulate in the cell walls, where it subsequently diffuses from the epidermis into the stele, or out of the root entirely<sup>12</sup>. Consequently, auxin concentration in the epidermis decreases rapidly with increasing distance from the apical auxin source. Since *aux1* plants accumulate a lower concentration of auxin in the root tip<sup>29</sup> and transport through the root cap is likely to be reduced<sup>12, 19</sup>, the supply of auxin to the elongation zone may also be decreased. The simulation shown in Fig. 4c assumes that the auxin supply to the elongation zone is reduced compared to wild type. If the auxin supply is unchanged (Fig. 4d), auxin concentrations in the *aux1* epidermis are uniformly higher, but still drop below the wild-type values ~500  $\mu\text{M}$  from the meristem. This may represent auxin distribution in the *wer/myb23* mutant, in which AUX1 is detected in the stele and the root cap, but not the epidermis. In both versions of the model hair cells in the differentiation zone (>500  $\mu\text{m}$  from the meristem) are supplied with less auxin if AUX1 is not expressed in non-hair cell files. This is because auxin taken into non-hair cells through the activity of AUX1 is returned to the cell wall further up the root by PIN proteins and becomes available to more distant hair and non-hair cells. This is in contrast to animal systems where increasing the morphogen uptake capacity of cells within a developing tissue reduces the amount available to more distant target cells<sup>30</sup>. An interesting consequence of this mechanism of auxin delivery is that hair cells can be supplied with auxin at an increased distance from the root tip without encountering high intracellular auxin concentrations. Variations to the model assumptions, including weak expression of *AUX1* in hair cells, or axial localization of *AUX1*, did not change the qualitative conclusions (see Online Supplementary Information).

Direct measurement of the intracellular concentration of auxin in hair and non-hair cells is not possible at present. We therefore used plants carrying the auxin-responsive reporter *DR5::GFP* to establish an assay for auxin accumulation. Following 4 hours' incubation with a 1  $\mu\text{M}$  auxin solution (indole-acetic acid), GFP signal in hair and non-hair cells was detected and quantified. The intensity of GFP signal was higher in wild-type non-hair cells than in wild-type hair cells, but no difference in the intensity of GFP signal was detected between hair and non-hair cells in the *aux1-22* mutant (Fig. 5a,b). Furthermore, the intensity of GFP signal in non-hair cells in the *aux1-22* mutant was lower than the intensity of GFP signal in non-hair cells of wild-type plants (Fig. 5a,b). These results are qualitatively consistent with the model prediction that non-hair cells accumulate a higher concentration of auxin than hair cells as a result of *AUX1* expression. Since *DR5::GFP* is an auxin-response reporter rather than a direct reporter of auxin concentration, the significance of the quantitative discrepancy between the 10-fold predicted difference in auxin concentration and the observed 1.6-fold difference in GFP expression is unclear. The sensitivity and specificity of the auxin response is dependent on the expression and interaction of components of the

auxin-signalling pathway and varies according to developmental context<sup>31</sup>. It will be interesting to identify whether such differences exist between hair- and non-hair cells and to investigate how *DR5::GFP* expression relates to the hair-specific auxin response.

Assuming auxin concentration over a threshold is required for root-hair growth, the model auxin concentrations predict that root hairs will cease to elongate closer to the root tip in *aux1-22* than in wild type. The length of the differentiation zone, measured as the distance between the first and the last elongating hair within a cell file, was found to be reduced in *aux1-22* plants compared to wild type (Fig. 5c). Furthermore, a positive correlation was observed between average root-hair length and the length of the differentiation zone amongst *aux1-22* plants (Fig. 5d). *aux1-22* root hairs were not found to grow at a significantly different rate to wild-type root hairs (Fig. S7) suggesting duration of growth, as determined by the length of the differentiation zone, is likely to account for the difference in root-hair length. This supports the model-based hypothesis that AUX1 is required to sustain delivery of root-hair promoting auxin to hair cells as they develop and increase in distance from the root tip.

The involvement of cell-type specific AUX1 expression in root-hair development highlights salient consequences of non-homogeneous auxin influx on auxin distribution in the root. Demonstration that AUX1 expression is required to deliver auxin to the differentiation zone endorses the finding that in addition to subcellular PIN localization<sup>3</sup>, tissue-specific AUX1 expression affects the movement of auxin between the epidermis and the underlying tissues and the longitudinal distance over which auxin is carried in the epidermis<sup>12</sup>. The effect of non-hair cell specific AUX1 expression on the auxin content of adjacent hair cells also demonstrates that AUX1 affects the auxin content not only of cells it is expressed in, but of surrounding cells as well. Previous models assume that auxin flows uniformly throughout the epidermis<sup>3,12</sup>. We show that this is not the case and provide an example of how this affects development of an agronomically important cell type.

## Materials and Methods

### Plant growth conditions

*AUX1::AUX1-YFP*<sup>21</sup>, *IAA2::uidA* auxin reporters<sup>19</sup>, lines used in the *HA-AUX1* transactivation experiment<sup>12</sup>, *UAS::axr3*<sup>12</sup> and *wer/myb23*<sup>23</sup> have been described previously. Driver lines *J0491* and *J2301* were obtained from the Nottingham Arabidopsis Stock Centre. *PIN2::PIN2-GFP*<sup>22</sup> was a kind gift from Dr. C. Luschnig. For phenotyping, plants were grown on solid growth medium<sup>32</sup> for 5 days. For laser confocal microscopy and measurement of root-hair elongation rate, seeds were grown for 5 days beneath a thin film of solid growth medium on a glass coverslip sealed within a humid chamber. All plants were grown under a regime of 16 hours light, 8 hours dark.

### Microscopy

Slides were immersed in 20 µg/mL solution of Propidium Iodide for one hour, and mounted directly onto the microscope stage of a Leica DM IRBE laser confocal microscope. Excitation was provided using a 488 nm laser and RSP500 mirror. Emission was measured between 500-520 nm for GFP and between 515-550 for YFP. The position of epidermal cells with respect to underlying cortical cells was determined by focusing deeper into the specimen and observing the position of underlying cortical cells. Positioning of epidermal cells was further confirmed by converting the z-stack into a 3D projection, from which transverse sections were viewed using Leica Deblur image software.

## Root-hair measurements

For root-hair length measurements, images were taken from above the root using a Leica MZFLIII microscope and Spot 2.2.1 (Diagnostic Instruments Inc.) camera. Lengths were obtained from photographs using Image J (<http://rsb.info.nih.gov/ij/>). The length of 10 hairs were measured from each plant. Growth rate was measured by imaging growing root hairs every 30 seconds for a total of ten minutes using a Leica DMIRE2 microscope and Leica DFC350FX camera. Measurements were made only of hairs greater than 50  $\mu\text{m}$  and less than 100  $\mu\text{m}$  in length in order to ensure that images represented the period of tip growth. The length of the differentiation zone was determined by subtracting the distance between the first epidermal cell upon which a hair was visible and the root tip, from the distance between the last growing hair in the same file and the root tip. At least two files per root were observed. Growing root hairs were identified by their characteristic morphology.

## GUS Histochemical staining

Five-day-old roots were immersed in staining solution (100 mM Sodium Phosphate, 10 mM EDTA, 0.5 mM Potassium Ferrocyanide, 0.5 mM Potassium Ferricyanide, 0.1 % Triton X-100, 0.5 mM X-GlcA) and incubated in the dark at 37 °C for 5 hours. Roots were imaged before and after staining using a Leica MZFLIII microscope and Spot 2.2.1 camera (Diagnostic Instruments Inc.).

## Computer model

A description of the computer model of auxin transport in the Arabidopsis root is contained in the Supplementary Information online.

## Supplementary Material

Refer to Web version on PubMed Central for supplementary material.

## Acknowledgments

We thank Prof. J. Schiefelbein for sharing material before publication, and Prof. Alan Champneys and Dr. Robert Payne for insightful discussions. ARJ was supported by a BBSRC studentship awarded to CML and CSG, and KK by a BBSRC Case Award to HMOL and CSG. The project was aided by travel funding for EK through the Centre for Plant Integrative Biology, which is a BBSRC/EPSRC Centre for Integrative Systems Biology.

## References

1. Sabatini S, et al. An auxin-dependent distal organizer of pattern and polarity in the Arabidopsis root. *Cell*. 1999; 99:463–472. [PubMed: 10589675]
2. Blilou I, et al. The PIN auxin efflux facilitator network controls growth and patterning in Arabidopsis roots. *Nature*. 2005; 433:39–44. [PubMed: 15635403]
3. Grieneisen VA, Xu J, Maree AF, Hogeweg P, Scheres B. Auxin transport is sufficient to generate a maximum and gradient guiding root growth. *Nature*. 2007; 449:1008–1013. [PubMed: 17960234]
4. Knox K, Grierson CS, Leyser O. AXR3 and SHY2 interact to regulate root hair development. *Development*. 2003; 130:5769–5777. [PubMed: 14534134]
5. Grebe M, et al. Cell polarity signaling in Arabidopsis involves a BFA-sensitive auxin influx pathway. *Curr. Biol*. 2002; 12:329–34. [PubMed: 11864575]
6. Fischer U, et al. Vectorial information for Arabidopsis planar polarity is mediated by combined AUX1, EIN2, and GNOM activity. *Curr. Biol*. 2006; 16:2143–2149. [PubMed: 17084699]
7. Masucci JD, Schiefelbein JW. The *rhd6* Mutation of Arabidopsis thaliana Alters Root-Hair Initiation through an Auxin- and Ethylene-Associated Process. *Plant Physiol*. 1994; 106:1335–1346. [PubMed: 12232412]

8. Pitts RJ, Cernac A, Estelle M. Auxin and ethylene promote root hair elongation in Arabidopsis. *Plant J.* 1998; 16:553–560. [PubMed: 10036773]
9. Rahman A, et al. Auxin and ethylene response interactions during Arabidopsis root hair development dissected by auxin influx modulators. *Plant Physiol.* 2002; 130:1908–1917. [PubMed: 12481073]
10. Lee SH, Cho HT. PINOID positively regulates auxin efflux in Arabidopsis root hair cells and tobacco cells. *Plant Cell.* 2006; 18:1604–1616. [PubMed: 16731587]
11. Cho M, Lee SH, Cho H-T. P-Glycoprotein4 Displays Auxin Efflux Transporter Like Action in Arabidopsis Root Hair Cells and Tobacco Cells. *Plant Cell.* 2007; 19:3930–3943. [PubMed: 18156217]
12. Swarup R, et al. Root gravitropism requires lateral root cap and epidermal cells for transport and response to a mobile auxin signal. *Nat. Cell Biol.* 2005; 7:1057–1065. [PubMed: 16244669]
13. Lynch JP. Roots of the Second Green Revolution. *Aust. J. Bot.* 2007; 55:493–512.
14. Kramer EM, Bennett MJ. Auxin transport: a field in flux. *Trends Plant Sci.* 2006; 11:382–386. [PubMed: 16839804]
15. Kramer EM. PIN and AUX/LAX proteins: their role in auxin accumulation. *Trends Plant Sci.* 2004; 9:578–582. [PubMed: 15564124]
16. Petrasek J, et al. PIN proteins perform a rate-limiting function in cellular auxin efflux. *Science.* 2006; 312:914–918. [PubMed: 16601150]
17. Wisniewska J. Polar PIN localization directs auxin flow in plants. *Science.* 2006; 312:883. [PubMed: 16601151]
18. Bandyopadhyay A, et al. Interactions of PIN and PGP auxin transport mechanisms. *Biochem. Soc. Trans.* 2007; 35:137–141. [PubMed: 17233620]
19. Swarup R, et al. Localization of the auxin permease AUX1 suggests two functionally distinct hormone transport pathways operate in the Arabidopsis root apex. *Genes Dev.* 2001; 15:2648–2653. [PubMed: 11641271]
20. Kleine-Vehn J, Dhonukshe P, Swarup R, Bennett M, Friml J. Subcellular trafficking of the Arabidopsis auxin influx carrier AUX1 uses a novel pathway distinct from PIN1. *Plant Cell.* 2006; 18:3171–3181. [PubMed: 17114355]
21. Swarup R, et al. Structure-function analysis of the presumptive Arabidopsis auxin permease AUX1. *Plant Cell.* 2004; 16:3069–3083. [PubMed: 15486104]
22. Abas L, et al. Intracellular trafficking and proteolysis of the Arabidopsis auxin-efflux facilitator PIN2 are involved in root gravitropism. *Nat. Cell Biol.* 2006; 8:249–256. [PubMed: 16489343]
23. Dinneny JR, et al. Cell Identity Mediates the Response of Arabidopsis Roots to Abiotic Stress. *Science.* 320:942–945. [PubMed: 18436742]
24. Lee MM, Schiefelbein J. Cell pattern in the Arabidopsis root epidermis determined by lateral inhibition with feedback. *Plant Cell.* 2002; 14:611–618. [PubMed: 11910008]
25. Leyser HMO, Pickett FB, Dharmasiri S, Estelle M. Mutations in the AXR3 gene of Arabidopsis result in altered auxin response including ectopic expression from the SAUR-AC1 promoter. *Plant J.* 1996; 10:403–413. [PubMed: 8811856]
26. Berger F, Haseloff J, Schiefelbein J, Dolan L. Positional information in root epidermis is defined during embryogenesis and acts in domains with strict boundaries. *Curr. Biol.* 1998; 8:421–430. [PubMed: 9550701]
27. Santelia D, et al. MDR-like ABC transporter AtPGP4 is involved in auxin-mediated lateral root and root hair development. *FEBS Lett.* 2005; 579:5399–5406. [PubMed: 16198350]
28. Kramer E. How far can a molecule of weak acid travel in the apoplast or xylem? *Plant Phys.* 2006; 141:1233–1236. [PubMed: 16896235]
29. Marchant A, et al. AUX1 Promotes Lateral Root Formation by Facilitating Indole-3-Acetic Acid Distribution between Sink and Source Tissues in the Arabidopsis Seedling. *Plant Cell.* 2002; 14:589–597. [PubMed: 11910006]
30. Fischer JA, Eun SH, Doolan BT. Endocytosis, Endosome Trafficking, and the Regulation of Drosophila Development. *Ann. Rev. Cell Dev. Biol.* 2006; 22:181–206. [PubMed: 16776558]

31. Teale WD, Papanov IA, Palme K. Auxin in action: signalling, transport and the control of plant growth and development. *Nat. Rev. Mol. Biol.* 2006; 11:847–859. [PubMed: 16990790]
32. Grierson CS, Roberts K, Feldmann KA, Dolan L. The COW1 Locus of Arabidopsis Acts after RHD2, and in Parallel with RHD3 and TIP1, to Determine the Shape, Rate of Elongation, and Number of Root Hairs Produced from Each Site of Hair Formation. *Plant Physiol.* 1997; 115:981–990. [PubMed: 9390433]



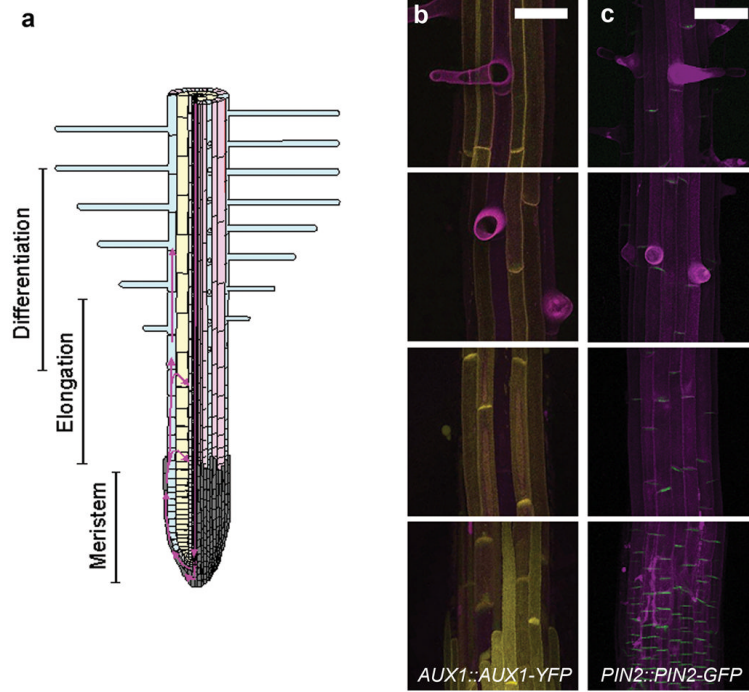


**Figure 1. AUX1 and PIN2 expression in hair and non-hair epidermal cells**

(a) Schematic diagram showing tissue organization and developmental zones of the Arabidopsis root. The left-hand side shows a longitudinal section. The right-hand side of the image shows a surface view of the root. Note that the differentiation zone overlaps the proximal end of the elongation zone. Root-hair cell files are shown in blue and non-hair cell files in pink. The root cap is shown in grey. Direction of auxin flow is shown in magenta<sup>2</sup>. (b-c) Confocal fluorescent imaging of auxin transporters in the developing root. From top to bottom images are representative of the expression pattern in the late differentiation zone, early differentiation zone, elongation zone and root cap. Cell walls are stained with propidium iodide (magenta). Scale bars represent 50  $\mu\text{m}$ . (b) Expression of *AUX1::AUX1-YFP* (yellow). (c) Expression of *PIN2::PIN2-GFP* (green).



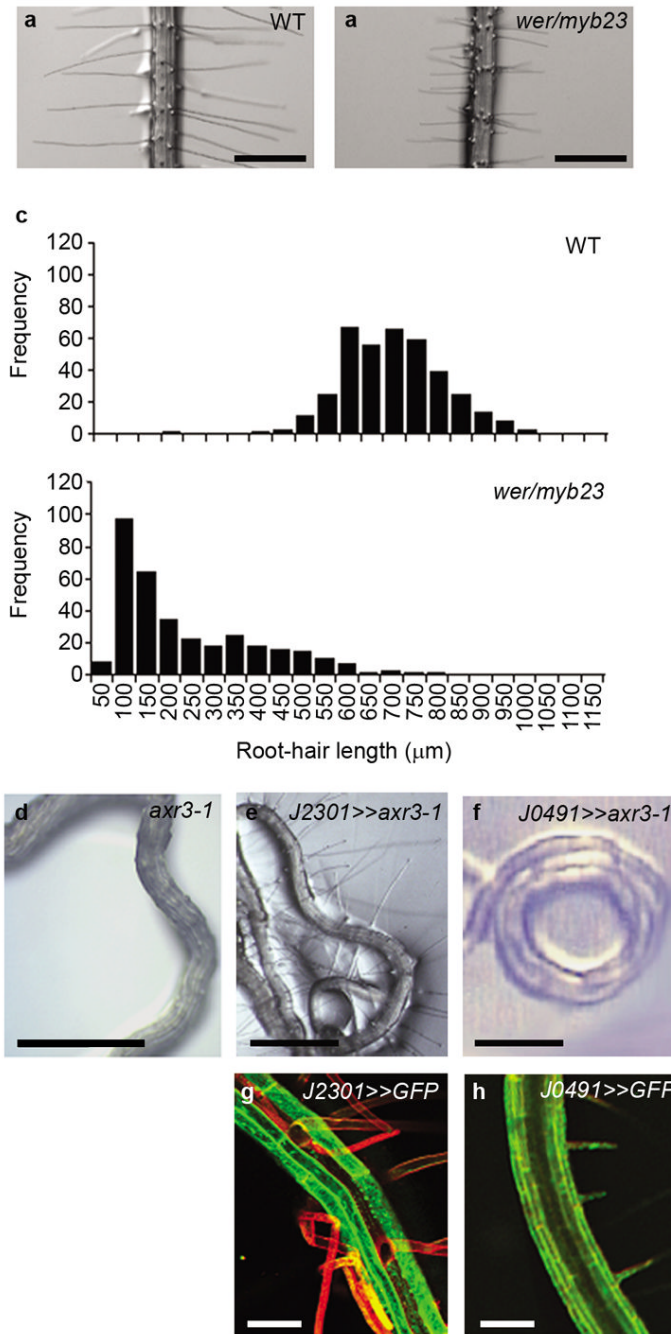


**Figure 3. Non-hair cells are essential for root-hair development, but an auxin response is not required in non-hair cells**  
**(a-b)** Root-hair phenotype of **(a)** wild-type and **(b)** *wer/myb23* plants. Scale bars represent 500 μm. **(c)** Frequency distribution of root-hair lengths in wild-type and *wer/myb23* plants. **(d-h)** Disruption of the auxin response through tissue-specific expression of *axr3-1* using a transactivation approach. **(d)** Root-hair-less phenotype of *axr3-1*. Root-hair phenotype of **(e)** *J2301>>axr3-1* and **(f)** *J0491>>axr3-1* F1 individuals. Scale bars represent 800 μm. **(g and h)** Expression pattern of the *J2301* and *J0491* promoters respectively as demonstrated by GFP expression. GFP fluorescence is shown in green. Propidium iodide stained cell walls

are shown in red. J2301 is expressed in non-hair cells, J0491 is expressed throughout the root. Scale bars represent 50  $\mu\text{m}$ .

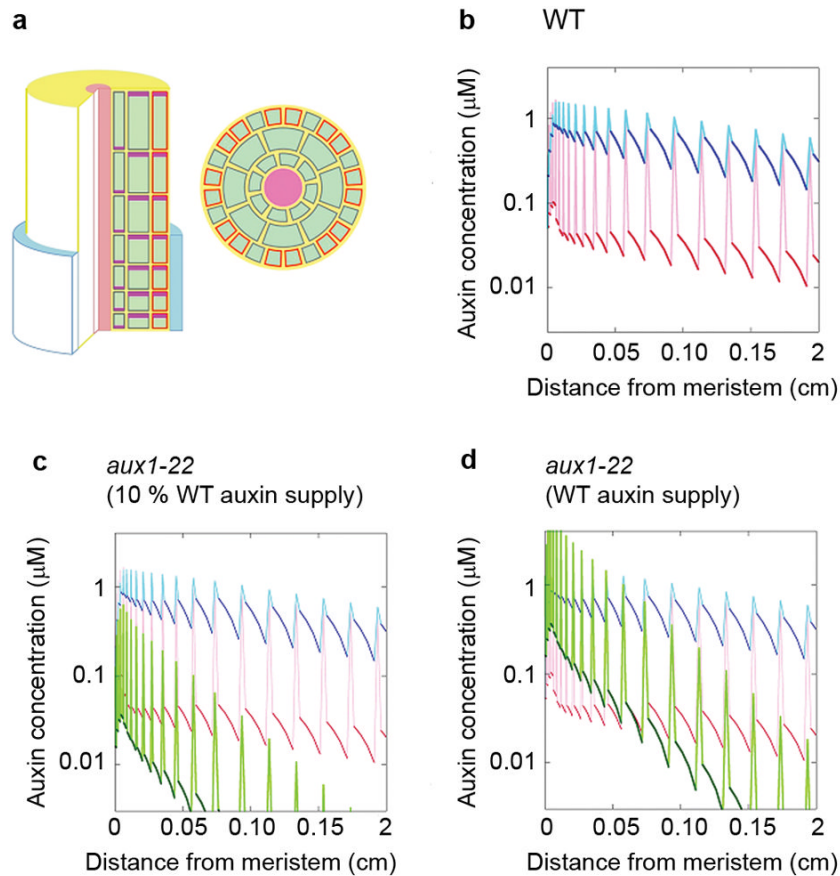


**Figure 4. Expression of AUX1 in non-hair cells affects the supply of auxin to hair cells in the differentiation zone of the root**

(a) The left-hand image shows a sketch of the computer model of the Arabidopsis root apex. The epidermis, cortex, and endodermis are resolved in the elongation and differentiation zones. Auxin is supplied to the tissue by the proximal end of the lateral root cap (blue) and transported basipetally by the activity of *AUX1* influx carriers (orange) and *PIN* family efflux carriers (plum). Cell membranes without influx carriers are shown in grey. Auxin is free to diffuse through the apoplast (yellow), which forms a continuous compartment between cells, and through the cytoplasm of cells (green). The right-hand image shows a transverse section through the model root showing cell geometry. Cells overlying a junction between two cortical cells are hair (H) cells; cells that do not overlie a junction are non-hair cells (N). *AUX1* expression is limited to N cells. (b) Model results showing the concentration of auxin in N cell files (blue) and H cell files (red) over increasing distance from the root tip. Dark colours show cytoplasmic auxin concentration, lighter colours show the apoplastic concentration between cells in a longitudinal file. (c) Model results for the *aux1* mutant (green) superimposed on the wild-type results from panel b, assuming auxin supply from the cap is 10 % of wild-type. (d) Model results for the *aux1* mutant assuming that the auxin supply from the lateral root cap is unchanged from wild type.

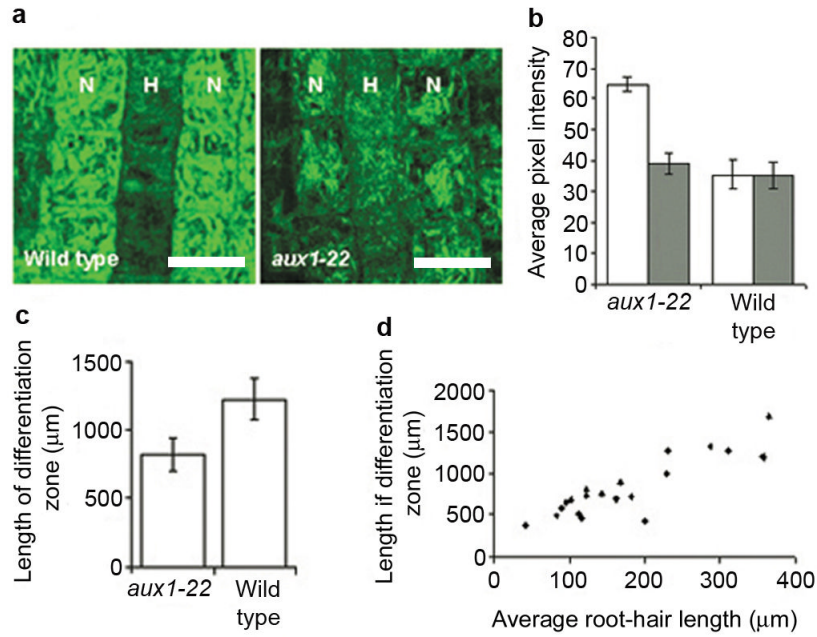


**Figure 5. *DR5::GFP* expression and root-hair growth dynamics support the model auxin distribution**

(a) Confocal fluorescent image of wild-type and *aux1-22* roots carrying *DR5::GFP* after 4 hours treatment with 1  $\mu$ M IAA. Non-hair cell files are indicated as N and hair-cell files are indicated as H. Scale bars represent 25  $\mu$ m. (b) Graph showing the average pixel intensity of GFP signal in wild-type and *aux1-22* plants expressing *DR5::GFP*. White bars represent non-hair cells, grey bars represent hair cells. Averages represent measurements from 4-6 roots. Error bars represent 95 % confidence intervals (n = 50-70 cells). (c) Average length of differentiation zone in wild type and *aux1-22*. Error bars indicate 95 % confidence intervals (n=20) (d) Relationship between average root-hair length and length of differentiation zone of *aux1-22* roots.